

Sabrina Marion · Nancy Guillen · Jean-Claude Bacri  
Claire Wilhelm

## Acto-myosin cytoskeleton dependent viscosity and shear-thinning behavior of the amoeba cytoplasm

Received: 2 August 2004 / Revised: 11 November 2004 / Accepted: 11 November 2004 / Published online: 12 February 2005  
© EBSA 2005

**Abstract** The mechanical behavior of the human parasite *Entamoeba histolytica* plays a major role in the invasive process of host tissues and vessels. In this study, we set up an intracellular rheological technique derived from magnetic tweezers to measure the viscoelastic properties within living amoebae. The experimental setup combines two magnetic fields at 90° from each other and is adapted to an inverted microscope, which allows monitoring of the rotation of pairs of magnetic phagosomes. We observe either the response of the phagosome pair to an instantaneous 45° rotation of the magnetic field or the response to a permanent uniform rotation of the field at a given frequency. By the first method, we concluded that the phagosome pairs experience a soft viscoelastic medium, represented by the same mechanical model previously described for the cytoplasm of *Dictyostelium discoideum* [Feneberg et al. in *Eur Biophys J* 30(4):284–294 2001]. By the second method, the permanent rotation of a pair allowed us to apply a constant shear rate and to calculate the apparent viscosity of the cytoplasm. As found for entangled polymers, the viscosity decreases with the shear rate applied (shear-thinning behavior) and exhibits a power-law-type thinning, with a corresponding exponent of 0.65. Treatment of amoeba with drugs that affect the actin polymer content demonstrated that the shear-thinning behavior of the cytoplasm depends on the presence of an intact actin cytoskeleton. These data present a physiologic relevance for *Entamoeba histolytica* virulence. The shear-thinning behavior could facilitate cytoplasm streamings during cell movement and cell deformation, under important shear experienced by the amoeba during the invasion of human tissues. In this study, we also investigated the

role of the actin-based motor myosin II and concluded that myosin II stiffens the F-actin gel in living parasites likely by its cross-linking activity.

**Keywords** Cytoplasm viscosity · Shear-thinning behavior · F-actin · Myosin II · *Entamoeba histolytica*

### Introduction

*Entamoeba histolytica* is a human parasite causing amoebic dysentery, a disease that is spread worldwide. This amoeba is a highly motile cell that invades the host intestinal tissue and reaches the blood circulation to disseminate towards other organs such as the liver. In this aspect, *E. histolytica* resembles cancer cells or neutrophils owing to its invasive properties into mammal tissues. Indeed, motility is a key activity for the virulence of the parasite. It has recently been shown that amoebae presenting a myosin II null phenotype, which is the main actin-based molecular motor for motility in *E. histolytica*, are defective to invade the liver and to form abscesses (Coudrier et al. 2004). During the process of tissue or microvasculature invasion, the amoebae undergo large deformations of the cell body and must withstand important mechanical shear.

During the last few decades, several studies focused on the mechanical properties of the cell cytoplasm and cortex in living cells, and developed original micromanipulation assays. These approaches are either based on cell deformation through manipulation of the cell surface, or on purely intracellular rheological methods. In the first case, the cell is aspirated in a micropipette or deformed between two microplates. The cortical cytoskeleton is constrained together with the cell's interior, which is then mostly characterized by the simple association of a viscosity and a spring. Micropipette aspiration assays were successful in measuring the cytoplasm viscosity of the whole cell under large deformations (Tsai et al. 1993). Interestingly, the cytoplasm viscosity

S. Marion · N. Guillen  
Unité de Biologie Cellulaire du Parasitisme, INSERM U389,  
Institut Pasteur, Paris, France

J.-C. Bacri · C. Wilhelm (✉)  
Laboratoire des Milieux Désordonnés et Hétérogènes,  
UMR7603, and FR2438 CNRS “Matière et Systèmes Complexes”,  
Université Pierre et Marie Curie, Paris, France  
E-mail: wilhelm@ccr.jussieu.fr

value was found to be shear-rate dependent, exhibiting shear-thinning behavior. Interestingly, pioneer work on actin filaments and microtubule suspensions has already demonstrated that the apparent viscosity decreases when the applied shear rate increases (Zaner et al. 1982; Buxbaum et al. 1987). The authors suggested that the flow property of these biologic polymer suspensions may explain certain aspects of cellular motility of living cells.

More recently, several studies have focused on intracellular microrheology techniques which allowed the probing of the viscoelastic properties of local regions in the cell cytoplasm and cortex. For instance, techniques using magnetic tweezers have been developed to probe the mechanical properties of macrophages (Bausch et al. 1999; Moller et al. 2000) and *Dictyostelium discoideum* (Feneberg et al. 2001). The prevalent model for cytoplasm rheological behavior deduced from these studies is a viscoelastic liquid. At short intervals (high frequency), the dynamics is dominated by elasticity, whereas at long intervals (low frequency), the medium behaves as a pure viscous liquid. These studies have also emphasized the role of the actin cytoskeleton and the microtubule network in the mechanical properties of the cell. *E. histolytica* appears as a simple system with regard to its intracellular organization. To date, conventional microscopic methods have provided no evidence for the existence of a microtubule network inside the cytoplasm. Furthermore, in contrast to mammalian cells, no clear endoplasmic reticulum network or central nuclear region can be defined in *E. histolytica*. During movement, nucleus and vesicles are transported within the cell by the cytoplasm flows. Interestingly, in this ancient protozoa, filamentous actin appears as the main polymer sustaining mechanical properties of the cell.

To investigate the mechanical properties of *E. histolytica*, we developed a magnetic-probe technique as a continuation of the application of magnetic tweezers. Our rotational microrheology method is based on the micromanipulation of magnetic phagosomes by an external magnetic field, allowing noninvasive quantification of local changes in the viscoelasticity of the cytoplasm. We focused our study on the mechanical response of the amoebic cytoplasm to a continuous deformation exerted by the rotation of a pair of magnetic beads. We observed that the cytoplasm viscosity is dependent on the shear rate applied (i.e., the frequency of the rotating magnetic field) and displays shear-thinning behavior. We demonstrated that the shear-thinning behavior followed a power law with a characteristic exponent of 0.65, almost similar to the value found for neutrophils (Tsai et al. 1993). The shear-thinning behavior of the cytoplasm tends to disappear in amoebae pretreated by latrunculin A, a compound that depolymerizes actin filaments. By contrast, the power-law exponent increased in the presence of jasplakinolide, a compound that enhances the actin polymer content. These data demonstrated for the first time in living cells that actin filaments are the main compounds inside the cell that account for the shear-thinning behavior of the

cytoplasm and correlated with the previous data obtained for pure actin polymer suspensions and for cells deformed in micropipette aspiration assays.

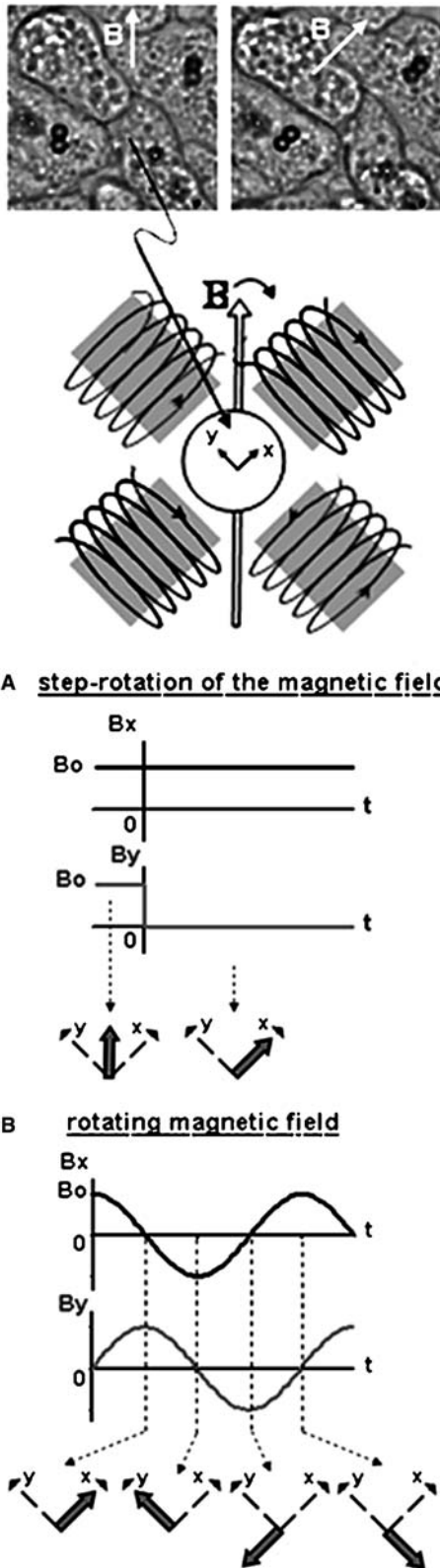
Furthermore, we investigated the role of myosin II, the main actin-based motor that sustains contractile activity at the rear pole and the cortex of the cell. We examined amoebae that overproduce the C-terminal coil-coil domain of the myosin II heavy chain [light meromyosin (LMM) fragment]. This fragment interacts with endogenous myosin II and thereby sequesters and inhibits the myosin II contractile activity. This strain displays a myosin II null phenotype characterized by a rounded cellular shape, drastically reduced movement, and failure to form uroids (Arhets et al. 1998). By the microrheology method that we developed, we showed that LMM+ amoebae exhibit an increase in the apparent cytoplasm viscosity compared with the control cells. These data show that myosin II stiffens the F-actin gel inside the cell cytoplasm and that in control amoebae the contractile activity may allow a gel-sol transition that renders the actin gel more liquidlike.

## Materials and methods

### Sample preparation

*Entamoeba histolytica* HM1:IMSS strain was cultivated axenically in TYI-S-33 medium at 37°C. The LMM+ cell line was generated as described later, according to Arhets et al. (1998). The DNA fragment encoding the end of the tail region of the myosin II heavy chain (LMM) was amplified by polymerase chain reaction from *E. histolytica* genomic DNA. The amplified DNA fragment was purified and cloned into the ExEhNeo vector (provided by E. Tannich, Bernhard Nocht Institute for Tropical Medicine, Hamburg, Germany). This vector also contains the gene conferring geneticin (G418) resistance as a selectable marker. The recombinant plasmid expressing LMM was introduced into *E. histolytica* by electroporation. Transfected amoebae were selected by incubation of cells in the presence of G418 at 10  $\mu\text{g ml}^{-1}$ . The available vectors for transfection of *E. histolytica* are maintained in the cell as episomal elements (Hamann et al. 1995). The transfected cell line, LMM-overexpressing cells, was routinely cultivated in the presence of 10  $\mu\text{g ml}^{-1}$  G418 in order to maintain a basic level of expression of the LMM fragment. Before each experiment, the LMM-overexpressing cells were grown for 72 h in the presence of 30  $\mu\text{g ml}^{-1}$  G418 in order to upregulate the expression of the transfected constructs.

The magnetic phagosomes were obtained by internalization of 2.8- $\mu\text{m}$ -diameter magnetic beads (Dynabeads M-280 tosyl-activated, Dyna) coated with human serum for 4 h. Amoebae containing magnetic beads were allowed to adhere (for 15 min at 37°C) on a glass dish positioned in the magnetic device adapted to the microscope (Marion et al. 2004). Depending on the



experiments, latrunculin A (0.1  $\mu\text{M}$ ) or jasplakinolide (10  $\mu\text{M}$ ) (Molecular Probes, Eugene, OR, USA) was added to the adherent amoebae for 15 min before viscoelasticity measurements.



**Fig. 1** The magnetic field setup illustrating the two configurations, which allow us the measurement of the viscoelasticity in living parasites. Two pairs of magnetic coils are adjusted within the horizontal plane around the measuring chamber and create a uniform magnetic field, on which the direction can be precisely imposed. **a** Transient response: the two pairs of coils are supplied with the same constant current, creating a static magnetic field  $\mathbf{B}$ , whose direction makes an angle of  $45^\circ$  with the  $x$  direction. Thanks to an electronic commutator, the current in the  $y$ -direction pair of coils is switched off at  $t=0$  within less than  $1\ \mu\text{s}$  and the field aligns with the  $x$  direction. **b** Permanent response: the two pairs of coils are supplied with alternating currents, displaying the same frequency  $F$ , but  $90^\circ$  out of phase. This creates a magnetic field vector, which rotates in the  $x$ - $y$  plane with always the same modulus and with a constant rotational velocity equal to  $2\pi F$ . The images in the *upper part* illustrate the alignment of magnetic phagosomes when submitted to the magnetic field  $\mathbf{B}$

### Magnetic probe

The rheological local measurements performed in this work involve the transient or permanent response of a bounded pair of magnetic phagosomes inside the amoebae when subjected to a rotating magnetic field. The motion of the pair is described with the angle  $\theta$  defining the pair direction and is governed by the angle  $\phi$  between the applied magnetic field and the direction of the pair, inducing a magnetic torque which tends to align the pair in the direction of the magnetic field. The measurement of the magnetization  $M(\mathbf{B})$  of the microbeads as a function of an applied magnetic field, performed using a Foner device, shows that the beads have paramagnetic behavior. Submitted to a magnetic field, phagosomes loaded with magnetic beads attract each other via dipole-dipole magnetic interaction and form cohesive pairs inside the cytoplasm (Fig. 1). Each magnetic bead (volume  $V$ ) of the pair carries an equal and parallel magnetic moment  $m(\mathbf{B}) = M(\mathbf{B})V$  when submitted to a magnetic field  $\mathbf{B}$ . The two beads interact via the energy of dipolar interaction  $U(\phi) = \frac{\mu_0}{24} M^2 V [1 - 3 \cos^2(\phi)]$  and the magnetic torque  $\Gamma_m$  exerted by the field on the pair directly:

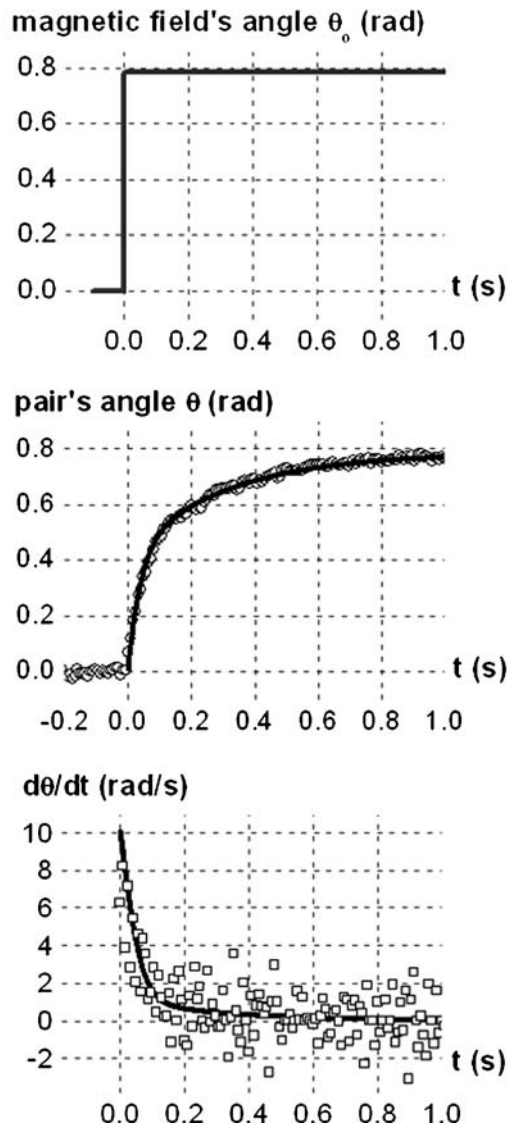
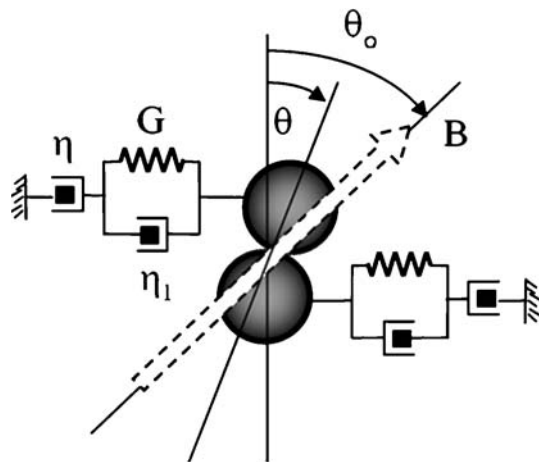
$$\Gamma_m = -\frac{dU}{d\phi} = -\frac{\mu_0}{8} M^2 V \sin(2\phi), \quad (1)$$

where  $\mu_0 = 4\pi \times 10^{-7}\ \text{A N}^{-2}$ .

The dynamics of the pair is then governed by the competition between this magnetic torque and the viscoelastic torque exerted by the surrounding medium, acting opposite to the direction of motion.

### The magnetic field device

We were able to apply a controlled magnetic torque on the pairs of phagosomes inside living amoebae. The experimental device consists of a set of four coils adapted to an inverted Leica microscope (Fig. 1), allowing us to produce a magnetic field  $\mathbf{B}$ , whose direction can be adjusted within the  $x$ - $y$  sample plane. The temperature is regulated at  $37^\circ\text{C}$  by the lens.



Our first approach to explore the local properties of the cytoplasm was to measure the response of an intracellular pair of phagosomes to a rotation step of the magnetic field. The two pairs of coils are then supplied



**Fig. 2** Transient response of a phagosome pair to a 45° rotation step of the magnetic field. **a** Mechanical representation of the *Entamoeba histolytica* viscoelastic cytoplasm. The simplest model to account for the viscoelasticity of the cell cytoplasm is the Kelvin–Maxwell model, represented by a viscous dashpot (viscosity  $\eta$ ) in series with an elastic element (elastic modulus  $G$  parallel to viscous dashpot  $\eta_1$ ). The viscoelasticity is probed through the rotation of a pair of magnetic phagosomes,  $\theta_0$  being the angle of the magnetic field and  $\theta$  the pair's angle at time  $t$ . **b** Instantaneous rotation of the magnetic field. **c, d** Typical creep rotational response curves for both the angle  $\theta$  (**c**) and its derivative  $d\theta/dt$  (**d**) for an intracellular pair of phagosomes. The response of the phagosome pair can be described in two steps, first with an immediate elastic jump followed by a viscous relaxation. Equation 2 allows us to fit (solid curve) the experimental data

with the same constant current, creating a static magnetic field, whose direction makes an angle of 45° with the  $x$  direction. The field can then align with the  $x$  direction within less than 1  $\mu$ s thanks to an electronic commutator (Fig. 1a). All the images were captured using an ultrafast camera and were digitized on a computer. The video system samples up to 500 images per second. In that condition, the number of sequences is sufficient to follow the motion of the pairs.

Our second approach was to measure the response of the pairs of phagosomes to a permanent rotation of the magnetic field, at a given frequency  $F$ . The magnetic field rotates if the two pairs of coils are supplied with an alternating current 90° out of phase (Fig. 1). Experimentally, the two pairs of coils positioned at right angles are powered by alternating currents displaying the same frequency but 90° out of phase (Fig. 1b). Therefore, the generated magnetic fields  $B_x$  and  $B_y$  are sinusoidal functions of time and both display the same frequency but with a phase shift of 90°. The resulting magnetic field is then constant in modulus, with a direction that rotates in the  $x$ – $y$  plane with the frequency of the currents applied. The motions of the pair are observed with a light microscope with a video-camera attachment and a recorder. Furthermore, the voltage signal is simultaneously fed to a light-emitting diode (LED), whose light intensity appears when  $B_x = 0$ . The angle of the magnetic field can then be derived for all captured frames.

#### Transient response: evaluation of the intracellular viscoelasticity

Creep experiments are performed by recording the rotation of a pair of magnetic phagosomes to a step rotation of the magnetic field applied (Fig. 2b). The pair rotation angle is measured on the captured frames using a self-written tracking algorithm implemented with the NIH image-processing software. Figure 2c shows single typical creep rotational response curve for an intracellular pair of phagosomes. The simplest model to account for the cell's interior viscoelasticity is the Maxwell model: a viscous dashpot (viscosity  $\eta$ ) in series with an elastic spring (elastic modulus  $G$ ). Here, the elastic fast response occurs with a nonzero characteristic time, and



a slight modification of the Maxwell model is necessary. The mechanical scheme presented in Fig. 2a is the simplest configuration that allows correct fitting for experimental curves (black lines in Fig. 2b, d). One must take into account that the same model has been found to describe the mechanical properties of the cytoplasm of amoeba *D. discoideum* (Feneberg et al. 2001).

The equation of motion of the pair is written as

$$\frac{\eta_1}{G} \frac{d^2\theta}{dt^2} + \frac{d\theta}{dt} = \frac{\Gamma_m}{\kappa V \eta} + \frac{1}{\kappa V G} \left(1 + \frac{\eta_1}{\eta}\right) \frac{d\Gamma_m}{dt}, \quad (2)$$

where  $\kappa$  is a geometrical factor.  $\kappa$  has been properly determined by following the 45° rotation of pairs of microbeads inserted in a well-calibrated Maxwell viscoelastic liquid. This fluid consists of surfactant molecules that form giant micelles in aqueous solutions (Wilhelm et al. 2003). It follows Maxwellian behavior (observed in a Couette rheometer), with a viscosity and relaxation times that can be modulated by decreasing temperature in the range 1–9 Pa s and 0.02–0.15 s, respectively. The viscosity  $\eta$  governs the long-time viscous behavior and the shear modulus  $G$  governs the initial fast elastic jump. The initial elastic response occurs with the characteristic time  $\tau_1 = \eta_1/G$ : the lower is the viscosity  $\eta_1$ , the faster is the jump.  $\tau = \eta/G$  is the time during which the medium shows elastic behavior, before becoming primarily viscous.

Permanent response: measurement of an effective viscosity at a given shear rate

We now consider the case when pairs of magnetic phagosomes are permanently rotated in a rotating magnetic field and are phase-locked to the field with a constant angle  $\phi$ . We then explore the viscous regime. Indeed, both shear rate and magnetic torque (varying as the sinus of the angle between the direction of the pair and the one of the field, as formulated in Eq. 1) are constant, that is:

$$\frac{d^2\theta}{dt^2} = 0 \quad \text{and} \quad \frac{d\Gamma_m}{dt} = 0. \quad (3)$$

This means that the motion of the pair is dominated by the viscous behavior of the medium surrounding the pair, and that the magnetic torque is only balanced by the viscous torque  $\Gamma_v$ :

$$\Gamma_v = -\kappa \eta V \frac{d\theta}{dt} = \Gamma_m = -\frac{\mu_0}{8} M^2 V \sin(2\phi), \quad (4)$$

$\eta$  being the viscosity and  $\kappa$  the geometrical factor. Once again,  $\kappa$  was calibrated by measuring the permanent rotation of pairs of beads inside the well-calibrated Maxwellian micellar solutions. This equation can also be seen as the limit of Eq. 2 when Eq. 3 is verified.

To resume this regime, the pair is embedded in a medium which suffers a constant applied shear rate  $\dot{\gamma}$

$$\dot{\gamma} = \frac{d\theta}{dt}, \quad (5)$$

and whose viscosity is given by

$$\eta = K \frac{\sin(2\phi)}{\dot{\gamma}}. \quad (6)$$

The coefficient  $K$  has been calculated from both the magnetic ( $M$ ) and geometric ( $\kappa$ ) characteristics:  $K = 0.782$  Pa. Practically, the phase angle  $\phi$  is deduced using the NIH software on captured frames by measuring the angle of the pair and subtracting it from the angle of the magnetic field (derived from the frame where the LED is switched on).

## Results

Viscoelastic behavior deduced from the creep response to a sudden torque

Creep experiments were performed inside amoebae with an intact F-actin cytoskeleton ( $n = 60$ ) or inside amoebae where actin filaments were depolymerized by latrunculin A treatment ( $n = 31$ ). In each case, the angular response curves exhibit two regimes: a fast elastic deflection followed by long-time viscous behavior, characteristic of viscoelastic liquids. The three viscoelastic parameters  $\eta$ ,  $G$ , and  $\eta_1$  were deduced in the two different conditions from each response curve by fitting Eq. 2 (see [Materials and methods](#)). Three different magnetic fields were applied to increase the initial magnetic torque and therefore the effective shear rate. We observe in parasites with an intact actin cytoskeleton, a slight dependence in the measured viscosity with the magnetic torque applied:  $\eta(B = 32.5 \text{ mT}) = 0.41 \pm 0.09 \text{ Pa s}$ ;  $\eta(B = 39 \text{ mT}) = 0.37 \pm 0.1 \text{ Pa s}$ ;  $\eta(B = 55 \text{ mT}) = 0.28 \pm 0.11 \text{ Pa s}$  (Fig. 3). This shear-thinning behavior disappears when actin filaments are depolymerized with latrunculin A and the measured viscosity drops for the three different magnetic fields, to  $\eta = 0.13 \pm 0.06 \text{ Pa s}$ . Interestingly, the elastic modulus  $G$  measured ( $G = 2.3 \pm 0.9 \text{ Pa}$ ) is not affected, either by the applied stress, or by the disruption of the actin filaments (Fig. 3). Nevertheless, one must be aware that for models describing the mechanical behavior of viscoelastic liquids by the association in series of an elastic component with a viscous one, the elastic modulus  $G$  represents only the high-frequency limit of the storage modulus. By contrast, the relaxation time  $\tau = \eta/G$  is the convenient parameter to quantify the extent of fluidlike versus solidlike behavior of the material: a purely elastic medium ( $\eta \rightarrow \infty$ ) is characterized by  $\tau \rightarrow \infty$ , whereas  $\tau = 0$  for a purely fluid medium ( $G \rightarrow \infty$ ). Inside amoebae with an intact actin cytoskeleton, the pairs of phagosomes are surrounded by a viscoelastic medium with relaxation time ranging from  $\tau(B = 55 \text{ mT}) = 0.14 \pm 0.03 \text{ s}$  to  $\tau(B = 32.5 \text{ mT}) = 0.19 \pm 0.03 \text{ s}$ . By contrast, when actin filaments were depolymerized, this relaxation time shortens in the same range of applied

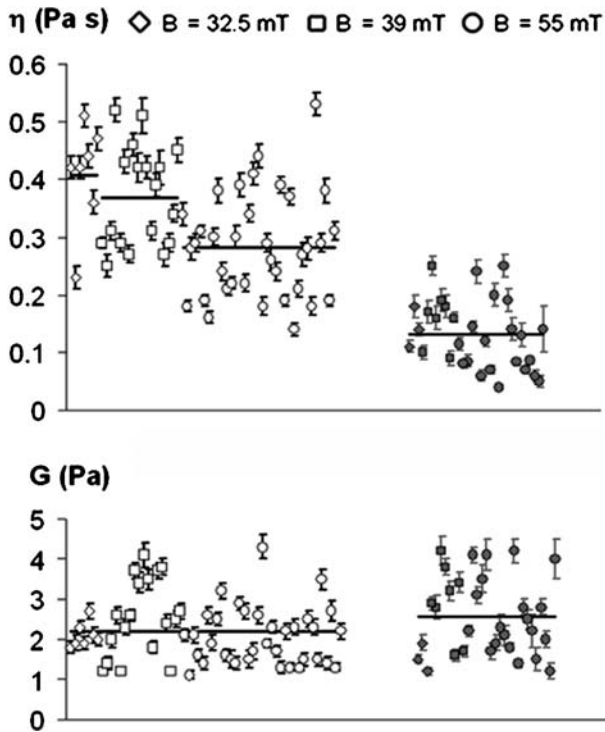


**Fig. 3** Viscoelastic parameters of the cytoplasm. Viscosity  $\eta$  and elasticity  $G$  deduced from each creep rotational response curve in amoebae with an intact cytoskeleton (*empty symbols*) and for amoebae pretreated with latrunculin A (*filled symbols*). Three different magnetic fields were applied. In parasites with intact F-actin cytoskeleton, the viscosity decreases when increasing the magnetic field  $B$  applied (that is the initial torque). This behavior disappears when actin filaments are depolymerized with latrunculin A. The elastic modulus  $G$  measured is affected neither by the applied stress, nor by the depolymerization of the actin filaments

torques:  $\tau = 0.06 \pm 0.03$  s. Together, these data demonstrate that the actin cytoskeleton accounts for a more solidlike behavior of the cytoplasm and also give evidence that the apparent cytoplasm viscosity inside living amoebae is shear-rate-dependent.

#### Viscosity measurement in a single cell at a given shear rate

At this stage of the experiments, we decided to focus on the measurement of the viscosity to explore the shear-thinning behavior previously observed in living parasites. Indeed, as observed in Fig. 2, the creep experiment does not allow us to fit experimental rotational curves with good accuracy in regard to the shear rate, especially in the viscous regime where the experimental shear rate  $\dot{\gamma} = \frac{d\theta}{dt}$  is not precise (Fig. 2c, d). In this case, the estimation of the viscoelasticity corresponds to first-approximation fitting, sufficient to model experimental points. By contrast, if the permanent rotation of a phagosome pair is imposed (phase-locked to the magnetic field), the medium sur-

rounding the pair suffers a constant shear rate  $\dot{\gamma}$ , exactly given by the angular frequency  $d\theta/dt = 2\pi F$ , where  $F$  is the frequency at which the magnetic field rotates (see [Materials and methods](#)).

First, we measured the cytoplasm viscosity following one phagosome pair that evolved in different local regions inside the amoeba. The translational motion of the pair was tracked for 22 s and the pair position was determined every 50 ms in each captured frame (typical frames are shown in Fig. 4a and the trajectory is shown in Fig. 4b). Simultaneously, the angle between the bead pair and the magnetic field is measured on each captured frame and the viscosity is derived from Eq. 3 for each position. First, we observed that the cytoplasm viscosity does not exhibit significant changes (measurement variations of about 8%) with the probe localization inside the cell (Fig. 4c). These data can be explained by the simple organization of the cytoplasm in *E. histolytica* that may display low micro-heterogeneity. Indeed, no microtubule network, actin stress fibers, or a central nuclear region are present in the cell cytoplasm.

Furthermore, to exclude the possibility that the shear-thinning behavior observed is the result of network destruction by shearing, we instantaneously dropped the rotation frequency (at  $t = 12$  s, Fig. 4c, arrow) to a value corresponding to 50% less than at the initial shear rate. We found that the viscosity immediately increased from  $0.20 \pm 0.008$  to  $0.30 \pm 0.01$  Pa s. This observation first confirms the previously observed shear-thinning behavior of the cytoplasm viscosity. It also clearly shows that the shearing history has no detectable effect on the measured viscosity of the cytoplasm. Indeed, if the intracellular gel was severely damaged by the shearing, decreasing the shear rate should not affect the measured viscosity of the modified gel. Therefore, we can conclude that the magnetic probe perturbs the microenvironment in a reversible manner, and in particular does not break the actin filaments irreversibly.

#### Global shear-thinning behavior for a cell population

We repeated the measurement of the cytoplasm viscosity for different shear rates in a whole population of parasites to further characterize the shear-thinning behavior previously observed. Figure 5 shows the variation of the viscosity as a function of the shear rate. For each shear rate examined, one plotted point represents the averaged measurement of the viscosity in many different amoebae (for instance, 335 amoebae probed at  $3.2 \text{ s}^{-1}$ ; 203 at  $1.6 \text{ s}^{-1}$ ). We found that the viscosity decreases with the shear rate  $\dot{\gamma}$  and therefore shows non-Newtonian behavior.

Furthermore, the mechanical behavior of the cytoplasm can be approximated as a power-law fluid, following



**Fig. 4** The local viscosity does not vary with the position of the probe inside the cell. **a** Image sequences showing the phagosome pair movement inside one particular adherent amoeba at different times, in the case of the permanent rotation of the magnetic field. **b** Corresponding tracking of the phagosome pair position for 22 s and every 50 ms. The magnetic field is rotated at the permanent frequency  $F=0.5$  Hz (empty symbols) and  $F=0.25$  Hz (filled symbols). **c** The angle between the phagosome pair and the magnetic field is measured at each capture frame and the viscosity value is then deduced using Eq. 5. At  $t=14.2$  s, a sudden drop in the rotation frequency from 0.5 to 0.25 Hz is applied (arrow). This corresponds to an immediate increase in the viscosity from 0.2 to 0.3 Pa s

examine the viscosity value at  $\dot{\gamma}_0 = 1 \text{ s}^{-1}$  in the following experiments.

#### Effect of drugs altering the actin cytoskeleton

A similar power-law model has been applied to describe most particulate and polymeric liquids over a remarkable range of shear rate (Bird et al. 1987). Therefore, we asked whether the actin filament polymers contribute to the mechanical properties of the cytoplasm, especially for the

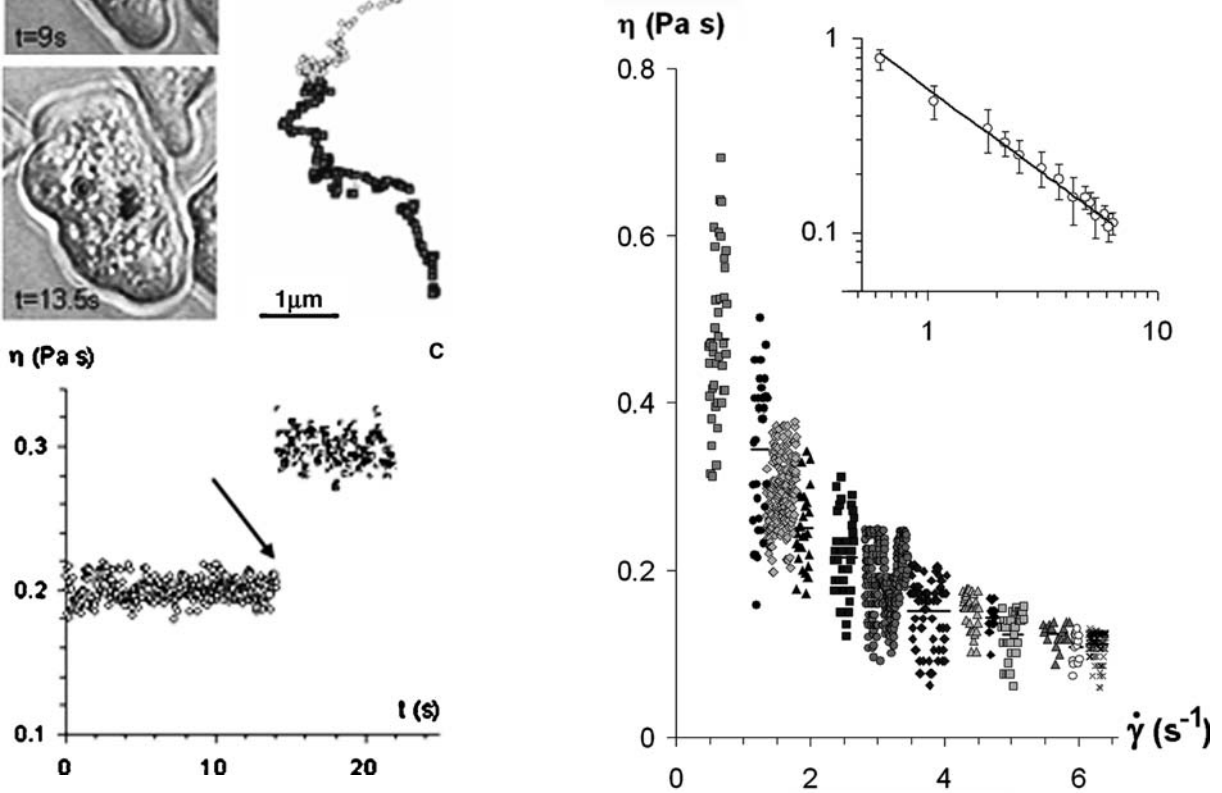


**Fig. 5** Shear-thinning behavior of the cytoplasm. Variation of the viscosity  $\eta$  as a function of the shear rate  $d\theta/dt$ . One given symbol corresponds to one given shear. For each shear rate examined, the viscosity is measured in several amoebae, each represented by a single symbol. *Inset*: viscosity as a function of shear rate on a log-log scale (one plotted point represents the averaged measurement of the viscosity in different amoebae for a given shear rate). The cytoplasm viscosity decreases with the shear rate  $\dot{\gamma}$ . The line corresponds to the fitting of the experimental data with Eq. 6

$$\eta(\dot{\gamma}) = \eta_0 \left( \frac{\dot{\gamma}}{\dot{\gamma}_0} \right)^{-\alpha}, \quad (7)$$

with a characteristic exponent  $\alpha = 0.65 \pm 0.02$ .

This power-law model fits the experimental results over 1 decade of the shear rates examined. At  $\dot{\gamma}_0 = 1 \text{ s}^{-1}$ ,  $\eta_0 = \eta(1 \text{ s}^{-1}) = 0.38 \pm 0.01 \text{ Pa s}$ . We chose to



shear-thinning behavior observed. We reproduced the same series of viscosity measurements in parasites preincubated for 15 min with latrunculin A or jasplakinolide. Latrunculin A treatment causes the massive depolymerization of actin filaments, which remain inside the cells as aggregates. By contrast, jasplakinolide treatment leads to a 4-times increase in the actin polymer content (Marion et al. 2004). We observed that the F-actin cytoskeleton organization inside the cytoplasm strongly influences the viscosity. Indeed, under conditions with a denser F-actin cytoskeleton (jasplakinolide treatment), the low shear-rate viscosity increases to  $\eta_0^{\text{jas}} = 0.58 \pm 0.02$  Pa s. By contrast, when the actin filament content is lower (latrunculin A treatment), the low-shear-rate viscosity decreases to  $\eta_0^{\text{lat}} = 0.18 \pm 0.01$  Pa s (Fig. 6a).

These data can be correlated to previous results obtained for actin polymer suspensions showing that the apparent viscosity in the power-law region is proportional to the polymer concentration (Zaner and Stossel 1982). Interestingly, when actin filaments are depolymerized before viscosity measurement, the shear-thinning behavior almost disappeared, with  $\alpha_{\text{lat}} = 0.32 \pm 0.04$ . By contrast,  $\alpha_{\text{jas}}$  increased to  $0.87 \pm 0.03$  when the actin filament content increased after jasplakinolide treatment. These data strongly suggest that actin filament polymers are the main compounds responsible for the shear-thinning behavior of the cytoplasm in *E. histolytica*.

#### Effect of myosin II on the viscosity of the cell cytoplasm

Myosin II is the major actin-based molecular motor that has been investigated for its role in cell motility and the cell's mechanical properties (Laevsky et al. 2003; Humphrey et al. 2002). It has been proposed that the contractile activity of myosin II promotes gel-sol transitions of the F-actin gel that would allow cytoplasm streaming in living cells (Janson et al. 1991; Kolega et al. 1991; Stossel 1993). Therefore, we investigated the role of myosin II for the mechanical properties of the cytoplasm in *E. histolytica*. We performed the same series of viscosity measurements inside parasites where endogenous myosin II contractile activity is inactivated by overexpressing the LMM fragment of the myosin II heavy chain (LMM+ cells) (Arhets et al. 1998). The overproduced LMM fragment interacts via its coil-coil domain with endogenous myosin II. It sequesters and thereby inhibits the contractile activity of the protein (Burns et al. 1995; Arhets et al. 1998).

First, we observed that the viscosity at low shear rate displays a twofold increase in LMM+ cells (Fig. 6b):  $\eta_0^{\text{LMM+}} = 0.71 \pm 0.03$  Pa s compared with  $\eta_0 = 0.38 \pm 0.01$  Pa s in control cells. The viscosity in LMM+ amoebae is increased for shear rates applied below  $3 \text{ s}^{-1}$ . This result shows that the overproduction of the LMM fragment stiffens the cell cytoplasm. Therefore, this result suggests that the contractile activity of myosin II participates in the mechanical properties of the cell cytoplasm and might be responsi-

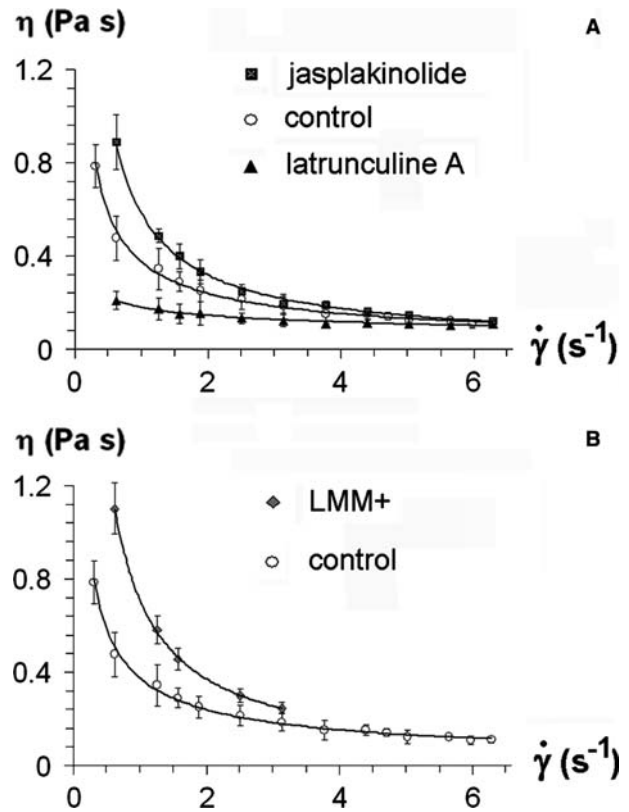


**Fig. 6** Acto-myosin cytoskeleton dependent viscosity as a function of shear rate. **a** The amoebae were pretreated with latrunculin A (triangles) or jasplakinolide (squares) to measure the viscosity under different shear rates. The low-shear-rate viscosity in control cells is  $\eta(0.62 \text{ s}^{-1}) = 0.48 \pm 0.05$  Pa s. When the F-actin cytoskeleton is denser (jasplakinolide treatment), the low-shear-rate viscosity increases to  $\eta(0.62 \text{ s}^{-1}) = 0.89 \pm 0.09$  Pa s. By contrast, when the actin filament content is lower (latrunculin A treatment), the low-shear-rate viscosity decreases to  $\eta(0.62 \text{ s}^{-1}) = 0.21 \pm 0.02$  Pa s. At high shear rate, the viscosity does not depend on the treatment with drugs:  $\eta(6.2 \text{ s}^{-1}) = 0.11 \pm 0.01$  Pa s. The curves represent the fitting using the power-law equation Eq. 6, with exponent  $\alpha = 0.65 \pm 0.02$  for control amoebae,  $\alpha = 0.87 \pm 0.03$  when cells are treated with jasplakinolide, and  $\alpha = 0.32 \pm 0.04$  when cells are treated with latrunculin A. **b** The same series of experiments with the LMM+ strain, inhibited for myosin II contractile activity (filled symbols). Again, the low-shear-rate viscosity increases to  $\eta(0.62 \text{ s}^{-1}) = 1.1 \pm 0.1$  Pa s. The curve represents the fitting using the power-law equation Eq. 6, with the exponent  $\alpha = 0.94 \pm 0.04$ .

ble, under normal motile conditions, for an active fluidization of the actin gel. The characteristic exponent  $\alpha$  also increases to  $\alpha_{\text{LMM+}} = 0.94 \pm 0.04$  so, when the shear rate increases, the viscosity value approaches more and more that measured in control cells, which can be shown as the high rate limit (see Discussion).

## Discussion

### Creep experiments

As a first step, we attempted to characterize the mechanical properties of the cytoplasm from



*E. histolytica*. To do that, we derived the intracellular magnetic tweezers technique (Bausch et al. 1999; Feneberg et al. 2001) in the rotating geometry and measured the transient response to an applied torque. We observed that the cell cytoplasm behaves as a viscoelastic liquid and that the rotational creep response curves can be fitted in a first approximation with a linear mechanical model. The cytoplasm can then be modeled with the same linear viscoelastic model used to describe the mechanical properties of *D. discoideum* cytoplasm (Feneberg et al. 2001). The cell interior seems to behave as a Newtonian body (the viscosity being constant with respect to the intensity of shearing). Nevertheless, one must be aware that, if the shear varies during the long-time viscous regime, we are not precise enough (Fig. 2d) in the angular measurement to correct the fitting with a shear-thinning law, limiting our fit to an average value for the viscosity in the range of the shear rate probed. However, if we increase the initial torque, the long-time viscosity decreases, revealing this time non-Newtonian shear-thinning behavior. We therefore focused on studying the long-time response to a constantly applied shear rate to explore the shear-thinning behavior and we chose to permanently rotate the pairs to work at the constant shear rate  $\dot{\gamma}$  imposed by the rotation of the magnetic field:  $\dot{\gamma} = d\theta/dt$ .

#### Shear-thinning behavior of the cytoplasm

Rheological properties of the cell have been extensively investigated through different techniques. For instance, the characterization of the mechanical properties of cortical cytoskeleton has been performed through binding of magnetic beads to focal adhesion sites and variation of the frequency of oscillation of the beads (Maksym et al. 2000). However, only micropipette aspiration assays give access to the behavior of the cell cytoplasm during long-time flow under shear, mimicking, to a certain extent, cell deformation in vivo. Interestingly, models in which the cytoplasm is represented by a simple Newtonian fluid did not fit the experimental data obtained in micropipette assays for large deformations. Indeed, a decrease in the viscosity of the cytoplasm has been reported, providing the first indication of shear-thinning behavior of the neutrophil cytoplasm (Tsai and coworkers 1993, 1997). Furthermore, the experiments revealed a power-law dependence of viscosity on shear rate with an exponent of 0.52. Nevertheless, micropipette assays allow us to apply the deformation only on the whole cell and through the surface. More recently, intracellular rheological techniques have been developed. Magnetic tweezers allowed us for the first time to deduce the local cytoplasm viscoelastic parameters through creep experiments (Bausch et al. 1999; Feneberg et al. 2001). With magnetic tweezers, the magnetic probe is translated at a given constant force and the viscosity can be directly deduced from the velocity over a long time. Nevertheless, the magnetic

probe continuously experiences a new microenvironment during its movement. By contrast, if the probe is rotated, we explore during the measurement the same zone, which experiences a permanent shear rate. Therefore, the technique we developed in this work derives from these previous pertinent studies but investigates for the first time the long-time viscous flow under constant, precisely determined intracellular shear.

The shear-thinning behavior observed in actin polymer gels could be generally thought to be the result of network destruction by shearing. However, we can exclude that the shearing perturbs the microenvironment irreversibly. Indeed, if the probe rotates at a high frequency, the sudden drop of 50% of the frequency is correlated with an immediate increase of the apparent viscosity (Fig. 4). Nevertheless, one must be aware that the permanent rotation of the magnetic probe locally reorganizes the F-actin network. Besides, in polymer systems, the shear thinning observed is mostly understood as a balance between disappearance and formation of entanglements between the chains, which suffer the shear flow (Watanabe 1999). In our experiments, it is probable that the network is partially, but reversibly, destroyed (disruption of low molecular interactions) and that the shear-thinning behavior reflects the capability of repairs during the cycle of probe rotation. Furthermore, *E. histolytica* is a highly motile cell in which, as in neutrophils, 80% of the actin is in monomer form (Marion et al. 2004) and no actin stress fibers are observed in the cytoplasm. Therefore, it could be envisioned that highly dynamic flows in the cytoplasm may constantly reorganize the microenvironment locally around the pair.

With the rotational rheological method we developed, we found by applying local shears inside the cell that in *E. histolytica* the cytoplasm behaves as a power-law fluid with an exponent  $\alpha = 0.65$ , almost similar to the one obtained in neutrophils (0.52) by micropipette aspiration assays.

#### Actin polymers are the main actors of the cytoplasm shear-thinning behavior

Similar power laws describing shear thinning in complex materials have been identified for the vast majority of entangled polymers (Watanabe 1999). The thinning occurs when the flow affects the global chain motion. This behavior can be satisfactorily predicted considering a balance of disappearance and formation of entanglements between the chains (Graessley 1967). Under an increasing shear flow, the molecules disentangle and the viscosity decreases. For synthetic polymers, in the shear-thinning region that fitted with a shear rate power-law dependence of the viscosity, the exponent increases with the concentration of polymers (Allain et al. 1997). The shear-rate dependence of the viscosity of the F-actin suspension was also confirmed and this dependence obeys the power-law relationship observed for entangled synthetic polymers (Zaner and Stossel 1982).

In a previous study, it was calculated that for an F-actin solution with an initial concentration of  $1 \text{ mg ml}^{-1}$ , the exponent is 0.67 (Zaner and Stossel 1982). Using our rotational rheological method, we also examined the apparent viscosity of an F-actin solution ( $0.5 \text{ mg ml}^{-1}$ ) at different shear rates and obtained an exponent of 0.48 (data not shown). This result also suggests that the exponent increases with the concentration of the polymers.

We observed that the shear-thinning behavior of the amoebic cytoplasm almost disappears when the cells are pretreated with latrunculin A, a drug that drastically decreases the actin polymer content. The data provided in this study demonstrate for the first time in living cells that the F-actin cytoskeleton contributes to a large extent to the viscosity parameter and in the shear-thinning behavior of the cytoplasm.

The power-law model we found fits the experimental results over about 1 decade of shear rates (Fig. 5). Interestingly, for high rates of shear, the measured viscosity ( $\eta = 0.1 \text{ Pa s}$ ) is similar in control cells and cells treated with drugs affecting the actin cytoskeleton, either increasing or decreasing the polymer content (Fig. 6a). It has already been predicted that the power-law model should fail at high shear rates, where the viscosity must ultimately approach a constant value: at high rates of shears, the molecules completely disentangle so that the viscosity is mainly a function of interactions between the polymer and the solvent. Presumably, we almost reach this high-shear-rate limit around  $6 \text{ s}^{-1}$ . Indeed, the viscosity values measured are then similar, independent of the F-actin drug treatments. This particular viscosity value could represent the participation of other cytosolic components, as vesicles, for the viscosity value of the cell's cytoplasm.

### Role of myosin II in the apparent viscosity of the cell cytoplasm

Previous work showed that the physical state of cross-linked actin gels critically depends on the concentration and the affinity of the cross-linker (Janmey and coworkers 1988, 1990; Wachsstock et al. 1994; Tseng et al. 2002). A gel cross-linked by purified filamin, a high-affinity F-actin binding protein, behaves like a stiff solid gel when the cross-linker is present in a high concentration (Janmey et al. 1990; Tseng et al. 2004). In contrast, in the presence of  $\alpha$ -actinin, or conventional myosin II, the F-actin gel behaves as a viscoelastic fluid (Wachsstock et al. 1994; Xu et al. 1998), which can be explained by the fact that these proteins are dynamic F-actin cross-linkers with a high dissociation rate (Humphrey et al. 2002). Myosin II is the actin-based molecular motor for cell motility and mechanical properties of the cell. Different conclusions have arisen from these previous studies. It was proposed that during cell motility, myosin II can act as an actin filament cross-linker, allowing the cell to exert a compressive force throughout

the cortex to balance the hydrostatic force from the extracellular medium. This hypothesis has been suggested recently because *D. discoideum* myosin II null mutants are defective in moving under restrictive environments, suggesting that the cell cortex is too flaccid to resist forces generated during movement (Shelden et al. 1995; Laevsky et al. 2003).

In addition, in amoeboid-type motility, myosin II contraction has been proposed as playing a crucial role for inducing gel-sol transitions of the actin gel to sustain cytoplasm streaming (Kogela et al. 1991; Janson et al. 1991). The molecular mechanism that could explain this activity has been investigated in vitro in pure F-actin gels (Humphrey et al. 2002). It has been shown that myosin II, in its inactive form, stiffens the gel by its cross-linking property. Upon activation of the contractile activity, the number of entangled filaments is reduced in the network by enhancing the longitudinal filament motion. In addition, it was suggested that during motility in amoeba, changes in actin-myosin II interaction during contractile activity can reduce the cortical stiffness in particular regions (lateral sides) and allow the extension of cell protrusions (Arhets et al. 1998). In the same way, when the invasive parasites undergo large deformations and suffer important shears, the contractile activity of myosin II in cell cytoplasm may facilitate cytoplasm streaming after pseudopod extension. However, such active fluidization of the cytoplasm has not been demonstrated in living cells.

Our results are in agreement with the proposed functions of myosin II. Indeed, we found that in the LMM+ strain, in which myosin II contractile activity is inhibited, the apparent viscosity increased to a large extent at low shear rates. This result suggests that inactivated myosin II molecules stiffen the cytoplasm likely by their F-actin cross-linking activity. Besides, the shear-thinning exponent for the LMM+ strain is close to 1 (0.94). Such an exponent has been found (Buxbaum et al. 1987) for actin and tubulin suspensions, where the shear-thinning behavior was interpreted as the critical rupture of the network under shear. We could therefore hypothesize that the cross-linking of the actin network induces a transition between the shear-thinning regime (with exponent 0.7) experienced by chains of polymers free to reorganize (Zaner and Stossel 1982) and the shear-thinning regime (with exponent 1), where the shear stress induces the critical rupture of the network (Buxbaum et al. 1987).

### Conclusion

The present work investigates for the first time the shear-thinning behavior of the amoeba cytoplasm, using intracellular local probes and application of well-determined shear rates.

The movement of migrating cells as fibroblasts is commonly described as proceeding in two steps. First, the cell extends a thin and large lamellipodia at the

leading edge and establishes new adhesion sites on the substrate. Next, the rear tail detaches from the substrate and is retracted via the contractile activity of myosin II. Amoeboid-like motility, in *E. histolytica* and neutrophils, presents morphological and molecular differences. It is not possible to distinguish a characteristic rear pole as observed in fibroblasts. The cell extends a thicker protrusion called pseudopodia, and the whole cell body is almost simultaneously propelled, thereby the movement appears more continuous. These cells are able to undergo large and dynamic deformations of the cell body, allowing an efficient migration under restrictive environments. The shear-thinning behavior observed in the cytoplasm of *E. histolytica* may play an important role in facilitating the motility of the parasite in human tissues. Indeed, if the cell extends faster at the leading edge than it contracts at the rear, this leads to local shears inside the cell cytoplasm. The shear-thinning behavior, together with the contractile activity of the cell cortex, would then allow the cell body to be rapidly propelled. This phenomenon is emphasized when cells suffer more important shears, as is the case when they enter small apertures in tissues or vessels during the invasive process.

## References

- Allain C, Cloitre M, Perrot P (1997) Experimental investigation and scaling law analysis of the swell in semi-dilute polymer solutions. *J Non-Newtonian Fluid Mech* 73:51–66
- Arhets P, Olivo JC, Gounon P, Sansonetti P, Guillen N (1998) Virulence and functions of myosin II are inhibited by overexpression of light meromyosin in *Entamoeba histolytica*. *Mol Biol Cell* 9(6):1537–1547
- Bausch AR, Moller W, Sackmann E (1999) Measurement of local viscoelasticity and forces in living cells by magnetic tweezers. *Biophys J* 76(1):573–579
- Bird RB, Armstrong RC, Hassager O (1987) Dynamics of polymeric liquids, vol 1. Fluid mechanics. Wiley, New York
- Burns CG, Reedy M, Heuser J, De Lozanne A (1995) Expression of light meromyosin in Dictyostelium blocks normal myosin II function. *J Cell Biol* 130(3):605–612
- Buxbaum RE, Dennerll T, Weiss S, Heidemann SR (1987) F-actin and microtubule suspensions as indeterminate fluids. *Science* 20235(4795):1511–1514
- Coudrier E, Amblard F, Zimmer C, Roux P, Olivo-Marín J-C, Rigotherier M-C, Guillen N (2004) Myosin II and the Gal-GalNAc lectin play a crucial role in tissue invasion by *Entamoeba histolytica*. *Cell Microbiol* (in press)
- Feneberg W, Westphal M, Sackmann E (2001) Dictyostelium cells' cytoplasm as an active viscoplastic body. *Eur Biophys J* 30(4):284–294
- Graessley W (1967) Viscosity of entangling polydispers polymers. *J Chem Phys* 47:1942–1953
- Hamann L, Nickel R, Tannich E (1995) Transfection and continuous expression of heterologous genes in the protozoan parasite *Entamoeba histolytica*. *Proc Natl Acad Sci USA* 92:8975–8979
- Humphrey D, Duggan C, Saha D, Smith D, Käs J (2002) Active fluidization of polymer networks through molecular motors. *Nature* 416:413–416
- Janmey PA, Hvidt S, Peetermans J, Lamb J, Ferry JD, Stossel TP (1988) Viscoelasticity of F-actin and F-actin/gelsolin complexes. *Biochemistry* 27:8218–8227
- Janmey PA, Hvidt S, Lamb J, Stossel TP (1990) Resemblance of actin-binding protein/actin gels to covalently crosslinked networks. *Nature* 345:89–92
- Janson LW, Kolega J, Taylor DL (1991) Modulation of contraction by gelation/solution in a reconstituted motile model. *J Cell Biol* 115:1479–1497
- Kolega J, Janson LW, Taylor DL (1991) The role of solution-concentration coupling in regulating stress fiber dynamics in nonmuscle cells. *J Cell Biol* 114:993–1003
- Laevsky G, Knecht DA (2003) Cross-linking of actin filaments by myosin II is a major contributor to cortical integrity and cell motility in restrictive environments. *J Cell Sci* 116(Pt18):3761–3770
- Maksym GN, Fabry B, Butler JP, Navajas D, Tschumperlin DJ, Laporte JD, Fredberg JJ (2000) Mechanical properties of cultured human airway smooth muscle cells from 0.05 to 0.4 Hz. *J Appl Physiol* 89(4):1619–1632
- Marion S, Wilhelm C, Voigt H, Bacri JC, Guillen N (2004) Overexpression of myosin IB in living *Entamoeba histolytica* enhances cytoplasm viscosity and reduces phagocytosis. *J Cell Sci* 117(Pt 15):3271–3279
- Moller W, Nemoto I, Matsuzaki T, Hofer T, Heyder J (2000) Magnetic phagosome motion in J774A.1 macrophages: influence of cytoskeletal drugs. *Biophys J* 79:720–730
- Shelden E, Knecht DA (1995) Mutants lacking myosin II cannot resist forces generated during multicellular morphogenesis. *J Cell Sci* 108(Pt 3):1105–1115
- Stossel TP (1993) On the crawling of animal cells. *Science* 260:1086–1094
- Tsai MA, Hammer DA (1997) Rheology of rat basophilic leukemia cells. *Ann Biomed Eng* 25(1):62–68
- Tsai MA, Frank RS, Waugh RE (1993) Passive mechanical behavior of human neutrophils: power-law fluid. *Biophys J* 65(5):2078–2088
- Tseng Y, Schafer BW, Almo SC, Wirtz D (2002) Functional synergy of actin filament cross-linking proteins. *J Biol Chem* 277:25609–25616
- Tseng Y, An MK, Esue O, Wirtz D (2004) The bimodal role of filamin in controlling the architecture and mechanics of F-actin network. *J Biol Chem* 279:1819–1826
- Wachsstock DH, Schwarz WH, Pollard TD (1994) Cross-linker dynamics determine the mechanical properties of actin gels. *Biophys J* 66:801–809
- Watanabe H (1999) Viscoelasticity and dynamics of entangled polymers. *Prog Polym Sci* 24(9):1253–1403
- Whilhelm C, Browaeys J, Ponton A, Bacri JC (2003) Rotational magnetic particles microrheology: the Maxwellian case. *Phys Review E* 67:061908
- Xu CJ, Wirtz D, Pollard TD (1998) Dynamic cross-linking by alpha-actinin determines the mechanical properties of actin filament networks. *J Biol Chem* 273:9570–9576
- Zaner KS, Stossel TP (1982) Some perspectives on the viscosity of actin filaments. *J Cell Biol* 93(3):987–991